大韓土木學會論文集
第13卷 第2號 · 1993年 5月
pp. 11~20

R/C 쌍곡 포물선 '안장' 쉘의 극한 거동 硏究

Investigation on R/C Hyperbolic Paraboloid (HP) Saddle Shell Ultimate Behavior

민창식* · 김생빈**
Min, Chang Shik · Kim, Saeng Bin

Abstract

Nonlinear inelastic behavior of an HP saddle shell has been examined by a finite element computer program developed on a Cray Y-MP. The mesh convergence is studied using three progressively refined finite element mesh models, 16×16, 32×32 and 64×64, for the elastic and inelastic analyses. It is shown that the 32×32 mesh model gives a solution that is very close to that given by the 64×64 mesh model, thus, showing a convergence. The inelastic analysis shows that the shell has a tremendous capacity to redistribute the stresses. At the ultimate, the concrete cracks and the reinforcement yieldings are spread out all over the shell, indicating that the stress distribution in the shell is approaching that given by the classical membrane theory. The present computer program provides a very useful tool for evaluating the nonlinear ultimate behavior of concrete shells during the design process.

요 지

쌍곡 포물선 '안장' 쉘의 極限 擧動을 슈퍼 컴퓨터에 개발한 有限要素 컴퓨터 프로그램으로 硏究하였다. 잘게 자른 3 모델을(16×16, 32×32 과 64×64) 이용하여 彈性과 非彈性 해석으로 유한요소망(mesh)의 수렴관계를 연구하였으며, 해석 결과 32×32 모델의 解가 64×64 모델의 결과에 매우 가깝게 나타나서, 이 모델이 수렴하고 있음을 보여 주었다. 非彈性 해석 結果 '안장' 쉘이 상당한 應力 재분포 能力을 갖고 있었으며, 극한 상태에서 콘크리트의 균열과 철근의 항복이 전체 쉘에 걸쳐서 나타 났다. 이 현상에 따라 응력 분포가 고전적인 膜理論 (Membrane theory)의 결과에 접근하고 있음을 관찰할 수있었다. 개발된 컴퓨터 프로그램은 설계시에 콘크리트 쉘구조물의 비선형 극한거동을 산정하는데 매우 유용하게 사용될 수 있을 것이다.

1. Introduction

Reinforced concrete hyperbolic paraboloid (HP) saddle shells have the same advantage that is inherent to most shells, i.e., resisting the applied loads primarily by membrane stresses. The surface of an HP saddle shell can be generated by a system of two intersecting straight lines thus making the forms for the casting of concrete shells relatively easy. Interest in understanding the ulti-

* 정회원 · 제주대학교 해양토목공학과 전임강사
** 정회원 · 동국대학교 공과대학 토목공학과 교수

mate behaviors of HP saddle shells was accelerated by the collapse of a saddle shell roof in Cheyenne, Wyoming[8], in 1975, 15 years after its construction. Like for other kinds of reinforced concrete shell structures, there are almost no experimental studies for HP saddle shells. Major reasons for the scarcity of the experimental studies are problems in testing and in interpretation of the results due to the extreme thinness of the shells.[14]

Currently, reinforced concrete shells are designed using a pointwise limit design method[9,12] based on stresses obtained from membrane or linear elastic bending analysis.[1,2] The lower bound theorem of plasticity provides a possible basis for such design practice-elastic analysis and pointwise limit design-since the elastic analysis or membrane analysis gives an equilibrium solution. This practice is quite common in other reinforced concrete structures.[1] However, reinforced concrete is not an elastic-perfectly plastic material as in the theorem. In other types of structures, the present design practice has been confirmed through years of analysis, testing, and experience. For reinforced concrete shells or HP saddle shells we have not yet established a general applicability of such a design philosophy.

Several investigators[4,5,7,18,19] have studied the same saddle shell that was first studied by Lin and Scordelis.[16] Lin and Scordelis[16] modeled a quarter of the saddle shell using 48 triangular bending elements. Muller and Scordelis[18] modeled the same problem with 105 triangular elements and used a 25% higher concrete cracking strength than that used by Lin and Scordelis. Both for the elastic and inelastic analyses, the Muller and Scordelis results were quite different from the Lin and Scordelis results. For example, the elastic tip displacement due to dead load only, obtained by Muller and Scordelis, was 38% higher than that obtained by Lin and Scordelis, a difference that can be attributed to a relatively refined model used by Muller and Scordelis. Similar observations were also made by Lin[15] and Akbar and Gupta.[4] Akbar and Gupta[5] made an effort to establish the relationship between the membrane reinforcement design method for the shell[9,11] and the adequacy of the design based on the ultimate behavior of the shell. They reported ten cases of results by varying design parameters and concluded that the design method gives a lower bound on the ultimate load for the cases studied. Cervera et al.[7] used the same problem to show the performance of the developed finite element model, and argued that an objective method of defining the softening branch of the tensile model is necessary.

As we will see later, the results from each team are widely scattered. These variations can be attributed to the differences in the models used by each team. Among many differences, as we will show in the present study, the mesh size of the finite element model contributes most significantly to the behavior of the saddle shells. None of the previous teams performed a convergence study on the finite element mesh size because performing several analyses by successively refining finite element meshes would be practically impossible using the conventional mainframe computers. Nonlinear finite element analyses for such shells are computationally quite intensive.

In the present study a reinforced concrete shell finite element computer program is developed on a Cray Y-MP supercomputer at the North Carolina Supercomputing Center, North Carolina, USA. The use of the vector pipelined supercomputer made it possible to perform a mesh convergence study that showed a significant effect of the mesh size on the computed response of the HP saddle shell.

1.1 Descriptions of problem

The middle surface of a hyperbolic paraboloid saddle shell planned on a square 2a by 2a having a rise or sag s at the corners (Figure 1) is defined by the equation

$$z = \frac{s}{a^2} xy = k\ xy, \qquad (1)$$

in which $k = s/a^2$ is a constant which is called the warping. When subjected to a uniform vertical loading of $q = -p_z$ on the horizontal projections, accodring to the classical membrane theory, the shell develops a uniform membrane shear N_{xy}

given by[2]:

$$N_{xy} = \frac{p_z\ a^2}{2\ s}, \qquad (2)$$

in which p_z is a uniformly distributed vertical load- ing of horizontal projection acting on the shell. The other stresses, N_x and N_y are based on the boundary conditions and are often assumed to be zero.

The problem chose for this study is the HP saddle shell designed and analyzed by Lin and Scordelis[15,16] and later studied by other investigators. Table 1 shows the material properties of concrete and steel. The material properties are identical for all the previous investigators, except that Lin-Scordelis used 375 psi (26.4 kg/cm^2) for the cracking strength of the concrete, and the others have used 471 psi (33.1 kg/cm^2). General views, plans, elevations and shell reinforcements of the Lin-Scordelis HP saddle shell is shown in Figure 1. Figure 2 shows the reinforcement and location of the reinforcement for the edge beam.

1.2 Method of analysis

As stated above a finite element computer program for reinforced concrete shells is developed on the Cray Y-MP supercomputer. In addition to the supercomputing vector algorithms that were implemented, the present computer program discretized the 4-node superparametric shell elements into several concrete and steel layers to account for the effect of bending on the cracking of concrete and yielding of steel.[13,16] As did the original Akbar-Gupta program, the present computer program includes the rotating crack model proposed by Gupta and Akbar.[11] A selective integration algorithm[3,22] is used for calculating the

Table 1. Material properties

CONCRETE	
Modulus of elasticity,	E_c=3,330 ksi (E_c=2.34×10^5 kg/cm^2)
Compressive strength,	f_c'=3,000psi (σ_{ck}=211 kg/cm^2)
Poisson's ratio,	ν =0.15
Weight of density,	ω_c =150pcf (W=2.4 t/m^3)
Cracking strength,	f_r =471psi (σ_{ru}=33 kg/cm^2)
STEEL	
Modulus of elasticity,	E_s=29,000ksi (E_s=20.4×10^5 kg/cm^2)
Yield stress,	f_y =60ksi (σ_y=4222 kg/cm^2)

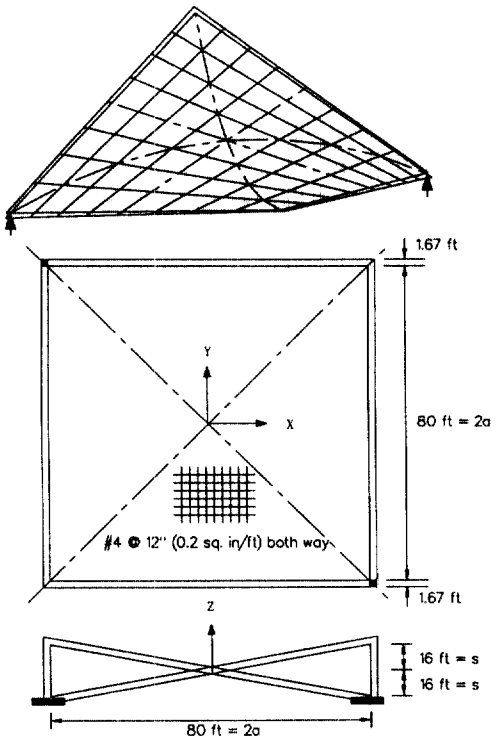

Fig. 1. The Lin-Scordelis HP saddle shell (ft× 0.3048=m, #4=SD13)

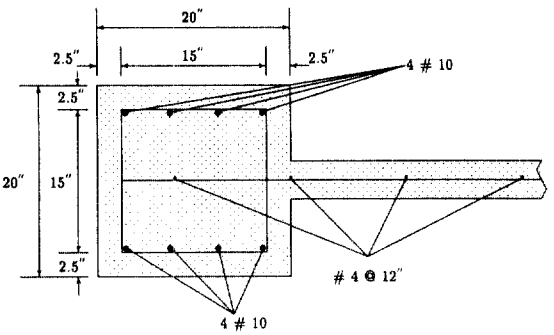

Fig. 2. The edge beam reinforcement (#10=SD 32, #4=SD13 reinforcement)

elastic stiffness matrix before cracking of concrete, and another selective integration algorithm is used to calculate the stiffness matrix of cracked concrete elements.[10] The biaxial behavior of uncracked concrete and the uniaxial behavior of the cracked element parallel to the cracks are assumed to be linear elastic in compression and in tension.

The shear retention factor(β) has been used widely by other investigators in the past.[6,13,16,18] Different investigators have used different values, and most of them have observed that the solution is insensitive to the numerical values of β in the range $1.0 \geq \beta > 0$. It has been pointed out by many researchers[6,13,16] that including a β factor improves the numerical stability of the solution process. With the present crack model[11] in which the crack direction is assumed to be perpendicular to the principal strain direction, theoretically, using a nonzero value of β should not change strains and stresses. As shown by Min and Gupta[17], the value of β does not change the behavior of the structure. In the present study we are using $\beta = 0.1$.

Reinforcing steel is assumed as an elastic-perfectly plastic material both in tension and compression, and is treated as a smeared equivalent uniaxial material. The finite element program is verified by nonlinear analysis on several example problems and by comparison with experimental results.[17]

1.3 Finite element model

We have studied the mesh convergence using three models. The first model is a 16×16 mesh model which was originally used by Akbar-Gupta. By successively subdividing, we generate a 32×32 mesh model and a 64 X 64 mesh model. The size of a square element goes down from 5 ft (152.4 cm) to 2.5 ft (76.2 cm) and then to 1.25 ft (38.1 cm). The edge beams are modeled as a single row of elements for all three models. Table 2 shows a summary of the finite element models with two types of element: single-layer membrane and multi-layer bending element.

2. Membrane shell analysis

2.1 Convergence study : elastic and inelastic analyses

We first start with the model which was originally used by Akbar and Gupta.[4] The shell is modeled by the membrane element that does not have any bending stiffness. This type of analysis was considered appropriate because an HP saddle shell resists the applied forces primarily through membrane stresses. To study the convergence among three mesh models, we obtain the results from the elastic analysis by applying dead load only. The vertical tip displacements vary widely from 0.19 ft (5.8 cm) to 0.35 ft (10.7 cm) and to 0.55 ft (16.8 cm) for the coarse to the refined mesh models. The numerical results from the three meshes do not show any sign of convergence as we refine the model from 16×16 to 32×32 and then to 64×64. From a practical stand point both the 32×32 and the 64×64 mesh models appear to be quite fine, and we expect that the two should give results that are quite close. A possible conclusion at this point would be that there is some-

Table 2. Parameters of the finite element models representing one quadrant of the shell

Model	16×16	32×32	64×64
Number of elements	89	305	1,121
Number of nodes	133	389	1,285
Number of degrees of freedom	336(448)*	1,056(1,536)*	3,648(5,637)*
Semi-bandwidth	87	167	327

* for the bending models

thing inherently wrong in the element and the overall model. That is the conclusion we finally reached as explained in the next section.

For the inelastic nonlinear analysis, 100% of the dead load is applied first followed by proportionally increasing live load. The convergence tolerance is taken to be 1% of the maximum applied nodal force at any load (displacement) step. As in the elastic analysis, the results from the inelastic analysis did not show any trend toward convergence either.[17] The crack and yield patterns of the shell from the models are inconclusive (not shown here). The present observation about the lack of convergence reinforces our earlier observation in conjunction with the elastic analysis. It appears that the problem with the model goes beyond the possible rigid body motion numerically introduced by weak supports. The present lack of convergence may be arising due to the lack of bending stiffness in the elements used to model the shell and the consequent formation of spurious mechanisms throughout the shell. As we will see later, the models that include the bending stiffness of the shell do converge rather nicely.

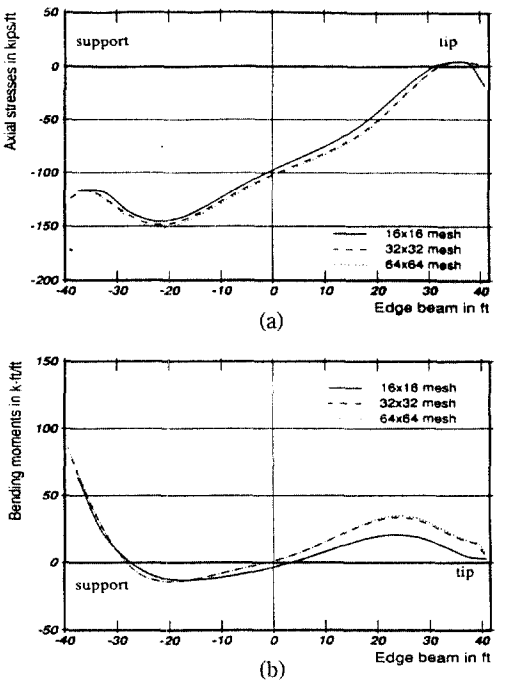

Fig. 3. Distributions of (a) axial stress (Kips/ft×1.49=t/m); (b) bending moment in the edge beam due to the dead load (k-ft/ft×0.454=t-m/m), bending models - elastic analysis

3. Bending shell analysis

We will now analyze the saddle shell including the bending stiffness in the elements both for the shell and the edge beams. For the bending finite element model, the edge beam elements are divided into ten concrete layers and three smeared reinforcement layers; and the shell elements are divided into ten concrete layers and one smeared reinforcement layer, both direction steels placed at the center of the cross-section.

3.1 Convergence study : elastic analysis

Only the dead load (50 psf=244 kg/m^2) of the structure is applied for the elastic convergence study, as in the membrane elastic analysis. The vertical tip displacements vary from 0.120 ft (3.66 cm) to 0.152 ft (4.63 cm) and to 0.157 ft (4.79 cm) for the coarse to the refined mesh models (16×16, 32×32, 64×64). Figures 3 (a) and (b) show comparisons of the axial stresses and the bending moments in the edge beam, respectively. The 32×32 mesh gives results that are very similar to those from the 64×64 mesh. The 16×16 mesh gives results that depart somewhat from the results of the refined meshes, but are not too bad. The only difference between the previous membrane elastic analysis and the present bending elastic analysis is that the former has bending stiffness in the edge beam and not in the shell elements, and the latter has bending stiffness both in the edge beam and the shell elements. The tip deflections from the membrane and the bending models clearly show that the lack of bending stiffness in the membrane element makes the shell too flexible.

3.2 Convergence study : inelastic analysis

Figure 4 shows the load-deflection curves obtained from the inelastic bending analysis using the

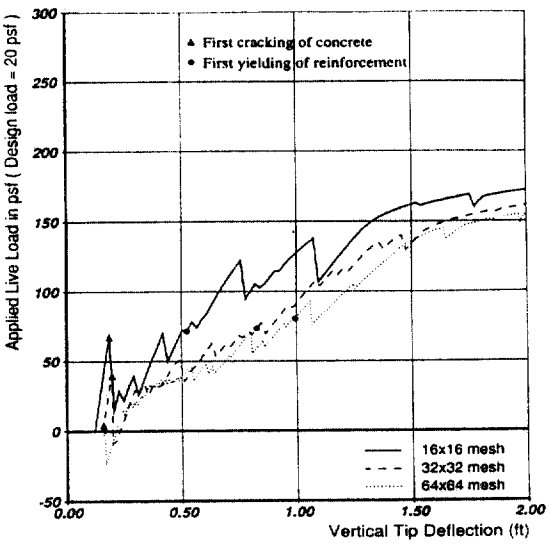

Fig. 4. Load-deflection curves for the bending models (psf×4.89=kg/m^2)

three mesh models. It also shows the occurrence of the initial concrete cracks and the initial reinforcement yieldings for the three models. The analyses are stopped after the models gained a relatively large vertical tip displacement, 2 ft (61 cm), without an apparent failure. The slope of the load-deflection curves toward the end is quite small. Therefore, the HP saddle shell must be close to failure. The present model does not consider the effect of large deformations. Therefore, it is considered prudent to not go beyond the present 2 ft tip displacement. The load resisted by the shell at the 2 ft tip displacement is taken to be the ultimate load, which is 172 psf (840 kg/m^2), 162 psf (792 kg/m^2) and 156 psf (762 kg/m^2) for the 16×16, the 32×32 and the 64×64 mesh models, respectively. When the model is refined from a 16×16 mesh to a 32×32 mesh, the ultimate load is decreased by 5.8%. When the model is refined from a 32×32 mesh to a 64×64 mesh, the ultimate load is decreased by 3.7%.

The load-deflection curves for the 32 X 32 mesh and the 64×64 mesh models reveal some loading stages with negative loads, which is unrealistic. This phenomenon happens because the present computer program uses the displacement increment drive.[17] When the shell develops a rather large number of initial cracks and consequently loses some of its stiffness quite suddenly, the computer program tries to find the matching load for the pre-defined displacement which does not exist in the real world. Thus, the computer program ends up picking a negative load for the equilibrium with that pre-defined displacement. The curves regain a positive load after a few more steps with increased displacement.

In Figure 4, the applied loads which cause the initial cracks are quite different for the three models, which indicates that an accurate representation of concrete cracks is highly dependent on the size of the mesh. As we refine the model, it can represent more accurately the peakness of the stresses and consequently can develop the initial cracks earlier. The live loads (psf) and the tip displacement (ft) at the initial yielding from the three models are: [72, 0.52] (351 kg/m^2, 15.8 cm), [73, 0.83] (357 kg/m^2, 25.3 cm), [80, 0.99] (391 kg/m^2, 30.2 cm). The reinforcement yielding is primarily governed by the inplane shear in the shell which is relatively uniform throughout the shell. Thus, refinement of the model does not change the distributions of the shear stresses (and the live load at which the initial yielding occurs) significantly. On the other hand, as we refine the model, more cracks are developed making the model more flexible and causing higher displacements at about the same applied load.

Figures 5 (a) and (b) show the distributions of the axial stresses and the bending moments in the edge beam at the ultimate, respectively. The distributions for the 16×16 mesh model are quite different from those for the other two models, particularly the moment distribution. On the other hand, the distributions for the 32×32 mesh model are very close to those for the 64×64 mesh model. Figures 6 and 7 show the crack patterns for the top concrete layer and the reinforcing steel yield patterns, respectively, for the three models at the ultimate. The figures show that the three models have similar crack and yield patterns.

4. Comparison with other results

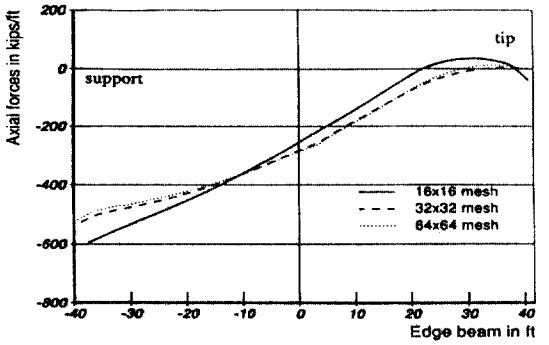

(a)

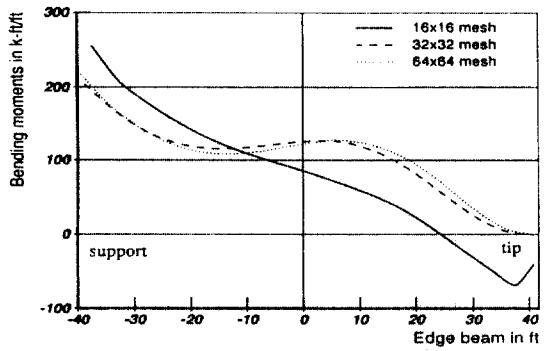

(b)

Fig. 5. Distributions of (a) axial stress; (b) bending moment in the edge beam at 2.0 ft vertical tip displacement, bending models - inelastic analysis

The HP saddle shell studied here was originally studied by Lin and Scordelis[16] and subsequently by several other investigators.[4,7,18] As discussed earlier, the results reported by Akbar and Gupta are obtained from a model that has a numerical problem associated with the lack of bending stiffness in the shell, which is not related to the actual behavior. Therefore, we drop the Akbar and Gupta [4] results from the comparison. The ultimate loads and the initial vertical tip displacement (due to dead load alone) predicted by various studies are given Table 3. The initial vertical tip displacements vary from 0.004 ft (0.12 cm) for Cervera et al to 0.157 ft (4.79 cm) for the present study. (We suspect that Cervera et al.[7] may have an error in printing. Their initial tip displacement is too small to be realistic.) As discussed earlier, the initial vertical tip displacement due to the dead load only is very sensitive to the mesh size. We did find that the mesh size is a major parameter influencing the behavior of the HP saddle shell because of rapid changes in stress-strain gradients near the edge beams.

The load factors in Table 3 are the ultimate applied live loads predicted by the nonlinear analysis divided by the design live load, 20 psf (97.7 kg/m^2). The load factors are more than 7.6 for all the analysis by the previous investigators, except Lin-Scordelis 5.5.[16] Figure 8 shows the load-deflection curves reported by the previous investigators and that obtained from the present

Table 3. Comparison of the ultimate and the initial vertical tip displacement from various studies

	Number of Elements	Element Type	Initial Vertical Tip Displacement, ft (cm)	Ultimate Load, psf(kg/m^2)	Load Factor*
Lin and Scordelis[16]	48	Triangle	0.104 (3.17)	110 (538)	5.5
Muller and Scordelis[18]	105	Triangle	0.14 (4.27)	163 (797)	8.1
Cervera et al.[7]	14	9-node	0.004 (0.12)	151 (738)	7.6
Present study	1,121	4-node	0.157 (4.79)	156 (762)	7.8

* ultimate applied live load / design live load, 20 psf (97.7 kg/m^2).

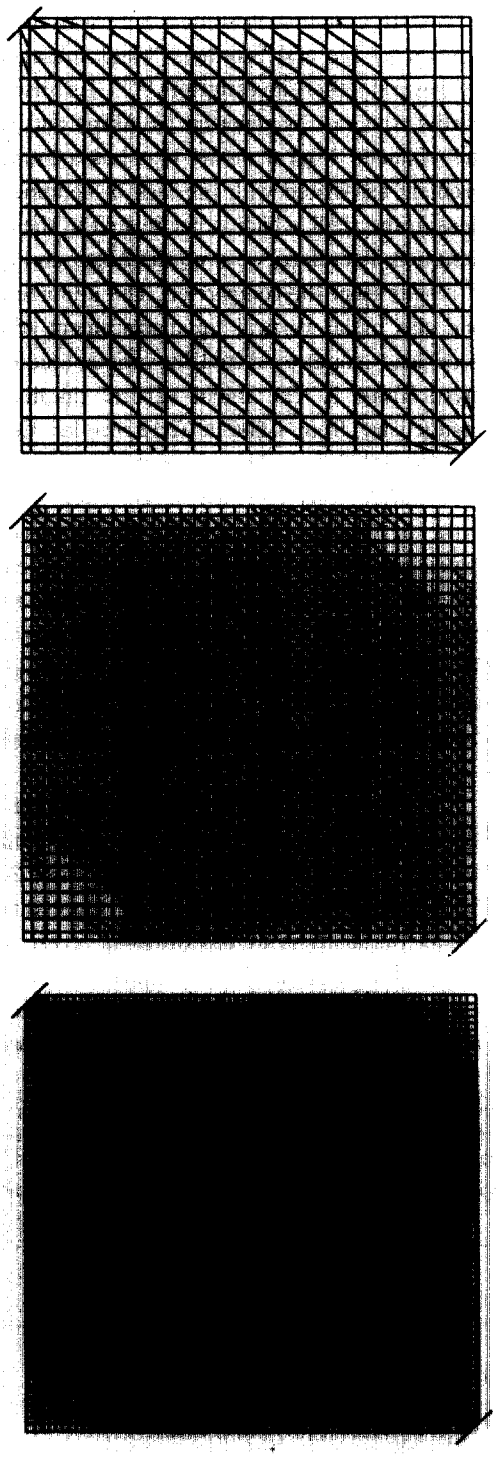

Fig. 6. Crack patterns in the top concrete layer at 2.0 ft vertical tip displacement in the bending models

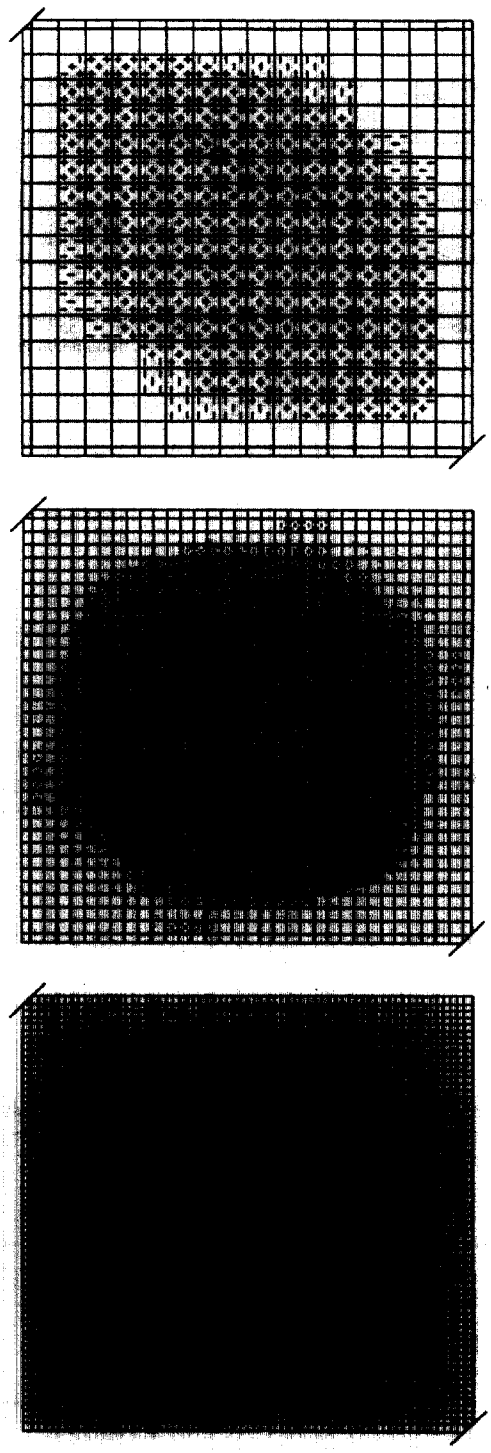

Fig. 7. Yield patterns at 2.0 ft vertical tip displacement in the bending models

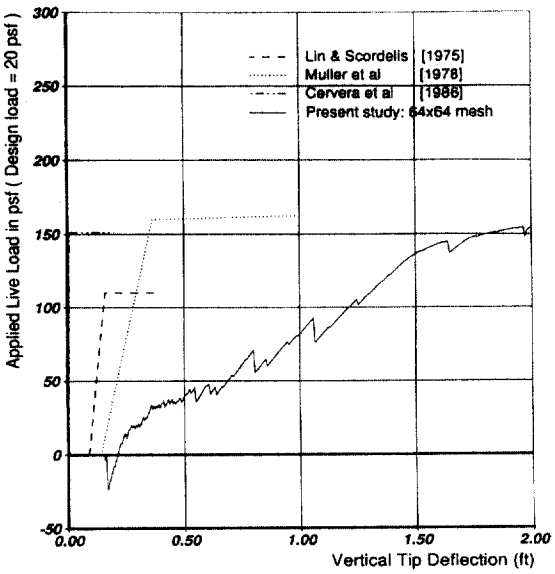

Fig. 8. Crack patterns in the top concrete layer at the applied live load (psf) and tip displacements (ft) of (a) [-23,0.17], (b) [34,0.4], (c) [47,0.67], and (d) [156,2.0] (psf×4.89=kg/m^2, ft×30.48=cm

bending analysis with the 64×64 mesh model. The load-deflection curve for the present bending analysis is different from all the other curves, even though the ultimate loads are quite close. The present bending analysis needs around 2 ft of vertical tip displacement to exert the ultimate stage. As suggested by Muller and Scordelis[18], the mesh size used by Lin and Scordelis[16] was too coarse to represent the HP saddle shell adequately. In the case of Cervera et al.,[7] the model has only ten 9-node elements for the shell, which is also very coarse. Then there is only the Muller and Scordelis[18] result left. We believe that a convergence study of the type reported here might bring the Muller-Scordelis and our results into closer agreement.

5. Conclusions

Ultimate behavior of the HP saddle shell under uniformly distributed vertical loading has been examined by inelastic finite element analyses using a 4-node superparametric membrane-bending shell element. We begin with the convergence study with the same element model used by Akbar and Gupta.[4] The shell is modeled by the membrane elements without bending stiffness, and the edge beams are modeled by the single-layer bending elements. As we refined the model from the 16×16 mesh to the 32 X 32 mesh and then to the 64×64 mesh, we were not able to achieve convergence among the meshes either for the elastic analysis or for the inelastic analysis. We later realized that the lack of bending stiffness in the elements used to model the shell may be causing numerical instabilities. As we introduced the multi-layer bending model, we successfully showed the convergence among the three mesh models both for the elastic and the inelastic analyses. The displacements and stresses from the 32×32 mesh model are very close to those from the 64×64 mesh model.

The inelastic analysis with the 64×64 mesh model shows that the shell has a tremendous capacity to redistribute the stresses through the membrane action. The ultimate load achieved by the 64×64 mesh is 156 psf (762 kg/m^2) (D+7.8L) at 2 ft (61 cm) vertical tip displacement. At the ultimate, the concrete cracks and the reinforcement yieldings are spread out practically all over the shell, indicating that the stress distribution in the shell is approaching that in the classical membrane theory. A comparison of the present results with the results by the previous investigators[4,7,16,18] shows the significance of the convergence study performed by us. The present computer program provides a very useful tool for evaluating the nonlinear ultimate behavior of concrete shells. It is possible for a designer to perform this type of an analysis on a routine basis-to assure structural strength and to accomplish economy in form and material.

References

1. ACI 318-89. Building Code Requirements for Reinforced Concrete (ACI 318-89). American Concrete Institute, Box 19150, Redford Station Det-

roit, Michigan 48219, (1989).
2. ACI. (1988). Hyperbolic Paraboloid Shells: State of the Art, American Concrete Institute, Prepared by ACI Committee 334 - Concrete Shell Design and Construction - Joint ACI-ASCE, SP-110.
3. Ahmad, Sohrabuddin, Irons, Bruce M., and Zienkiewicz, O. C. (1970). "Analysis of Thick and Thin Shell Structures by Curved Finite Elements." Int. J. for Numer. Meth. in Eng., 2, 419-451.
4. Akbar, Habibollah, and Gupta, Ajaya K. (1985). "Membrane Reinforcement in Concrete Shells: Design Versus Nonlinear Behavior." North Carolina State University, Raleigh, North Carolina 27695-7908, January. Reinforced Concrete Shell Research Report.
5. Akbar, H., and Gupta, Ajaya K. (1986). "Membrane Reinforcement in Saddle Shells: Design Versus Ultimate Behavior." J. Struct. Engrg., 112, 800-814, April.
6. ASCE. (1982). State-of-the-Art Report on Finite Element Analysis of Reinforced Concrete, Prepared by the Task Committee on Finite Element Analysis of Reinforced Concrete Structures of the Structural Division Committee on Concrete and Masonry Structures. American Society of Civil Engineers.
7. Cervera, M., Kent, A. J., and Hinton, E. (1986). "A Finite Element Model for the Nonlinear Analysis of Reinforced Concrete Shell Structures." In Shell and Spartial Structures: Computational Aspects, 315-328, Leuven, Belgium, July, Proceedings of the International Symposium: Lecture Notes in Engineering.
8. ENR. (1975). "15-year-old HP roof fails, injuring 18." Engineering News-Record, page 12, July.
9. Gupta, A. K. (1981). "Membrane Reinforcement in Shells." J. Struct. Div., ASCE, 107(1), 41-56.
10. Gupta, A. K., and Akbar, H. (1983). "A Finite Element for the Analysis of Reinforced Concrete Structures." Int. J. for Num. Meth. Eng., 19, 1705-1712.
11. Gupta, A. K., and Akbar, H. (1984a). "Cracking in Reinforced Concrete Analysis." J. Struct. Engrg., 110(8), 1735-1746.
12. Gupta, A. K., "Membrane Reinforcement in Concrete Shells: A Review." Nuclear Engineering and Design, 82, 63-75, (1984b).
13. Hand, Frank R., Pecknold, David A., and Schnobrich, William C., "Nonlinear Layered Analysis of RC Plates and Shells." J. Struct. Div., 99(7), 1491-1505, (1973).
14. Ketchum, Milo S., and Konkel, E. V., "Design of the Hanger Roof Structure of the TWA Overhaul Hangar, Kansas City." In Concrete Thin Shells, 149-166, SP-28, ACI, P.O. Box 4754, Detroit, Michigan 48219, (1971).
15. Lin, C. S., "Nonlinear Analysis of Reinforced Concrete Slabs and Shells." Technical report, University of California, Berkeley, California 94720, December, Report No. UC-SESM 73-7, (1973).
16. Lin, Cheng-Shung, and Scordelis, Alexander C., "Nonlinear Analysis of RC Shells of General Form," J. Struct. Div., 101(3), 523-538, (1975).
17. Min, Chang Shik, and Gupta, Ajaya K., "A Study of Inelastic Behavior of Reinforced Concrete Shells Using Supercomputers." Technical report, Department of Civil Engrg., North Carolina State Univ., Raleigh, North Carolina 27695-7908, March 1992. Reinforced Concrete Shell Research Report, (1992).
18. Muller, Guenter, and Scordelis, A. C., "Nonlinear Analysis of Reinforced Concrete Hyperbolic Paraboloid Shells." Technical report, University of California, Berkeley, California 94720, October, Report No. UC-SESM 77-6, (1977).
19. Muller, G., Kabir, A. F., and Scordelis, A. C., "Nonlinear Analysis of Reinforced Concrete Hyperbolic Paraboloid Shells." 191-203, Darmstudt, July 3-7 1978, Contributions to the IASS Symposium, Vol. 1, (1978).
20. Noor, Ahmed K., and Camin, Robert A., "Symmetric Consideration for Anisotropic Shells." Computer Methods in Applied Mechanics and Engineering, 9, 317-335, (1976).
21. Schnobrich, William C., "Analysis of Hipped Roof Hyperbolic Paraboloid Structures." J. Struct. Div., 98 (ST7), 1575-1583, (1972).
22. Zienkiewicz, O. C., Taylor, R. L., and Too, J. M., "Reduced Integration Technique in General Analysis of Plates and Shells." Int. J. for Num. Meth. Eng., 3, 275-290, (1971).

(接受 : 1993년 월 일)